



OPEN ACCESS

Open Access
Scan to access more
free content

Handling editor Tore K Kvien

► Additional material is published online only. To view please visit the journal online (<http://dx.doi.org/10.1136/annrheumdis-2015-207490>).

¹Nuffield Department of Orthopaedics, Rheumatology and Musculoskeletal Sciences, University of Oxford, Oxford, UK

²National Institute for Health Research Oxford Musculoskeletal Biomedical Research Unit, Oxford, UK

³National Institute for Health Research Oxford Comprehensive Biomedical Research Centre, Botnar Research Centre, Nuffield Orthopaedic Centre, Oxford, UK

⁴Division of Clinical Neurology, Nuffield Department of Clinical Neurosciences, John Radcliffe Hospital, University of Oxford, Oxford, UK

⁵Wellcome Trust Centre for Human Genetics, University of Oxford, Oxford, UK

Correspondence to

Professor B Paul Wordsworth, NIHR Oxford Musculoskeletal Biomedical Research Unit, Botnar Research Centre, Nuffield Orthopaedic Centre, Windmill Road, Headington, Oxford OX3 7LD, UK; paul.wordsworth@ndorms.ox.ac.uk

Received 20 February 2015

Accepted 19 August 2015

Published Online First

9 October 2015



CrossMark

To cite: Vecellio M, Roberts AR, Cohen CJ, et al. *Ann Rheum Dis* 2016;**75**:1534–1540.

EXTENDED REPORT

The genetic association of *RUNX3* with ankylosing spondylitis can be explained by allele-specific effects on IRF4 recruitment that alter gene expression

Matteo Vecellio,^{1,2,3} Amity R Roberts,^{1,2,3} Carla J Cohen,^{1,2,3} Adrian Cortes,^{4,5} Julian C Knight,⁵ Paul Bowness,^{1,2,3} B Paul Wordsworth^{1,2,3}

ABSTRACT

Objectives To identify the functional basis for the genetic association of single nucleotide polymorphisms (SNP), upstream of the *RUNX3* promoter, with ankylosing spondylitis (AS).

Methods We performed conditional analysis of genetic association data and used ENCODE data on chromatin remodelling and transcription factor (TF) binding sites to identify the primary AS-associated regulatory SNP in the *RUNX3* region. The functional effects of this SNP were tested in luciferase reporter assays. Its effects on TF binding were investigated by electrophoretic mobility gel shift assays and chromatin immunoprecipitation. *RUNX3* mRNA levels were compared in primary CD8+ T cells of AS risk and protective genotypes by real-time PCR.

Results The association of the *RUNX3* SNP *rs4648889* with AS ($p < 7.6 \times 10^{-14}$) was robust to conditioning on all other SNPs in this region. We identified a 2 kb putative regulatory element, upstream of *RUNX3*, containing *rs4648889*. In reporter gene constructs, the protective *rs4648889* 'G' allele increased luciferase activity ninefold but significantly less activity (4.3-fold) was seen with the AS risk 'A' allele ($p < 0.01$). The binding of Jurkat or CD8+ T-cell nuclear extracts to the risk allele was decreased and IRF4 recruitment was reduced. The AS-risk allele also affected H3K4Me1 histone methylation and associated with an allele-specific reduction in *RUNX3* mRNA ($p < 0.05$).

Conclusion We identified a regulatory region upstream of *RUNX3* that is modulated by *rs4648889*. The risk allele decreases TF binding (including IRF4) and reduces reporter activity and *RUNX3* expression. These findings may have important implications for understanding the role of T cells and other immune cells in AS.

INTRODUCTION

Ankylosing spondylitis (AS) is a common form of spondyloarthropathy (SpA) with numerous robust genetic associations, of which most are currently unexplained. Some functional protein-coding single nucleotide polymorphisms (SNPs) have been identified in genes associated with AS, such as *HLA-B*, *ERAP1* and *IL23R*.^{1–4} More commonly, the associated SNPs lie in non-coding flanking sequences or intragenic regions where they may influence gene expression.^{1 2 5} Genome-wide association studies (GWAS) show convincing association between *RUNX3* and AS and psoriatic arthritis, another form of SpA.^{1 2 6} This association extends to a cluster of SNPs at the *RUNX3* locus,¹ located from 0.5 to 2 kb

upstream of the *RUNX3* promoter. One of these, *rs4648889*, lies in a putative transcription regulatory region defined by DNaseI hypersensitivity and the presence of chromatin marks correlated with active enhancers (H3K4Me1 and H3K27Ac).⁷ *RUNX3* is a member of the runt domain-containing family of transcription factors (TFs), which play key roles in many developmental pathways.⁸ The *Runx3*^{-/-} mouse shows a complex phenotype affecting several organs, highlighting the broad spectrum of *RUNX3* action.⁹ *RUNX3* influences several types of immune cell that could be involved in AS, including natural killer (NK) cells and regulatory T cells,^{10 11} but seems particularly involved in the differentiation and development of CD8+ T cells.^{12 13} It seems relevant that CD8+ T-cell numbers are reduced in AS and that this is related to the *RUNX3* genotype.^{1 2} There is evidence for epigenetic regulation of *RUNX3* expression; the gene has two differentially expressed alternative promoters resulting in proteins that have dissimilar transcriptional activation capacity.^{14 15} The distal promoter is specifically demethylated in T cells¹⁶ but is methylated on both alleles in clonal cell populations.¹⁷ *RUNX3* promoter methylation status has also been incriminated in acute myeloid leukaemia¹⁸ and malignant transformation of ovarian endometriosis.¹⁹

Numerous SNPs in a ~15 kb linkage disequilibrium (LD) block upstream of *RUNX3* are strongly associated with AS. In the recent large ImmunoChip study, the lead SNP was *rs6600247* ($p = 1.3 \times 10^{-14}$), which is in complete LD with *rs4648889* (~2 kb upstream of the *RUNX3* promoter).¹ Here we apply conditional analysis to investigate the LD patterns within this region to identify the SNP(s) most likely to be primarily associated with AS. We also use historic ENCODE data on the transcriptional and epigenetic regulation of *RUNX3*,²⁰ together with in vitro and ex vivo molecular assays to investigate functional effects of *rs4648889* on *RUNX3* expression.

METHODS**Genotyping**

Historical typing data from the AS ImmunoChip study¹ were available for some patients or were otherwise obtained using TaqMan SNP assay (Life Technologies, Paisley, UK) to assign *rs4648889* genotypes. Where required, DNA was extracted using the Qiagen AllPrep DNA/RNA Mini Kit (Qiagen, Manchester, UK).

Imputation

Genotype data from the UK cases in the International Genetics of Ankylosing Spondylitis Consortium AS ImmunoChip study and WTCCC2 controls¹ were used to localise primary association signals. Haplotypes were inferred using SHAPEIT²¹ with default parameters. Untyped variants were imputed using haplotypes from phase III of the 1000 Genomes Project (October 2014 release)²² and using IMPUTE V2.²³ Association analysis with a Bayesian logistic model accounting for uncertainty in imputed variants (score method) was performed using SNPTEST.²⁴ Population structure was accounted for by including 10 principal components (PCs) as covariates in the regression analysis. Evidence for association is reported as the Bayes factor comparing the model of association with no association. The default priors in SNPTEST for the analysis were used.

Luciferase reporter assay

The 250 bp sequence flanking *rs4648889* was amplified from human genomic DNA and cloned into the TA cloning kit pCR2.1 vector (Invitrogen, Paisley, UK), then subcloned into the pGL4.23(luc2/minP) reporter vector (Promega, Madison, Wisconsin, USA) at the SacI/XhoI restriction sites (primer sequences available on request). Point mutations corresponding to genetic variants (G/A) of *rs4648889* were introduced using the QuikChange II XL Site-Directed Mutagenesis Kit (Agilent, Santa Clara, California, USA). Luciferase reporter assay details are available online (see online supplementary methods section).

Patients with AS

Following informed consent (COREC 06/Q1606/139 and OXREC B 07/Q1605/35), venous blood samples were obtained from 19 patients with positive HLA-B27 (average age 51 years, range 29–72) of white British ancestry fulfilling the modified New York criteria for AS.²⁵ Sixteen were taking non-steroidal anti-inflammatory analgesics, two were on sulfasalazine but none were currently taking corticosteroids or immunosuppressants. None of the cases had ever received biological therapy, but four with active disease were sampled immediately before starting biological therapy. Twelve cases had low disease activity (<4/10) measured by the Bath AS Disease Activity Index (BASDAI)²⁶ but overall there was a considerable range of disease activity (mean BASDAI 4.8/10, range 0.7–10) and C reactive protein (CRP) (mean 17 mg/L, range 0.5–74).

CD8+ T-cell isolation

CD8+ T cells were isolated from peripheral blood mononuclear cells using the CD8+ T-cell Isolation Kit (Miltenyi, Biscley, UK), according to manufacturer's instructions. CD8+ T cells were then plated for 4 h in RPMI supplemented with 10% fetal bovine serum before harvesting for experiments.

Electrophoretic mobility gel shift assay

Nuclear extract from Jurkat cells was prepared using the Thermo Scientific NE-PER Nuclear and Cytoplasmic Extraction kit (Thermo Scientific, Waltham, Massachusetts, USA). Electrophoretic mobility gel shift assays (EMSAs) were performed with LightShift Chemiluminescent EMSA Kit (Thermo Scientific, Waltham, Massachusetts, USA) using 5 µg of nuclear extract and 0.6 ng biotin-labelled double-stranded oligonucleotides (50 bp fragment—Eurofins, Wolverhampton, UK). The sequences of the synthetic single-stranded oligonucleotides used in the construction of these double-stranded oligonucleotides are listed in the online supplementary methods.

Probes were prepared using a biotin 3' end DNA labelling kit (Thermo Scientific, Waltham, Massachusetts, USA).

Single-stranded biotinylated oligonucleotides were mixed and annealed at room temperature for 1 h. Unlabelled competitor probes were used in 100-fold excess.

EMSAs were performed according to standard protocol (Thermo Scientific).

Band intensity was quantified with ImageJ software (Bethesda, Maryland, USA).

A detailed protocol is available online (see online supplementary methods section).

Chromatin immunoprecipitation—PCR

Chromatin immunoprecipitation (ChIP) was performed using the Diagenode Low Cell# ChIP kit (Liege, Belgium). For each ChIP, 6×10^4 CD8+ T cells were incubated with 1% formaldehyde for 10 min and 1.25 M glycine added for 5 min. DNA isolation was performed with DNA isolation buffer supplied by the kit. Quantitative PCR (qPCR) was performed on immune complex-associated DNA using allele-specific primers for *rs4648889* (common forward primer: 5'-CCCTACGTGCTTTG CTGTTT-3', AS risk 'A' allele reverse primer: 5'-GGGCCTGG ACTCAGGTGT-3', AS-protective 'G' allele reverse primer: 5'-GGGCCTGGACTCAGGTGC-3'), detected with SYBR Green on ABI ViiA7 PCR instruments (Applied Biosystems, Paisley, UK). A compensatory factor ($(\log(100)/\log 2)$) was subtracted from the cycle threshold (Ct) values of the diluted input (1%) in order to calculate the Ct values of the 100% input. Calculation of relative enrichment was done as follows: signals obtained from the ChIP are divided by signals obtained from input sample (representing the amount of the chromatin used in the ChIP) = $2^{\wedge}(\text{adj input-ct(IP)})$.

Relative occupancy was calculated as a ratio of specific signal over background: % input (specific loci)/% input (background loci).

The antibodies used were: IRF4 (Santa Cruz Biotechnology, Dallas, Texas, USA, sc-377383), H3K4Me1 (Diagenode, Liege, Belgium, C15200150) and IgG (Diagenode, Liege, Belgium, C15200001).

Quantitative real-time PCR

RNA was isolated with TRIzol (Invitrogen, Paisley, UK) and cDNA synthesis (for 500 ng RNA) was prepared with Superscript III from Invitrogen (Paisley, UK). A final concentration of 5 ng/µL was used in qPCR, which was performed with the ABI ViiA7 PCR instrument (Applied Biosystems, Paisley, UK) using SYBR Master mix (Applied Biosystems, Paisley, UK) with evaluation of dissociation curves. mRNA levels of each gene were quantified using the $\Delta\Delta\text{Ct}$ method and normalised to β -actin. For each gene, PCR melting curves were checked to evaluate the single, specific product.

The specific primers designed were RUNX3 forward: 5'-ACT CAG CAC CAC AAG CCA CT-3' RUNX3 reverse: 5'-GTC GGA GAA TGG GTT CAG TT-3' RUNX3 values were normalised to β -actin (Hs_ACTB_1_SG QuantiTect Primer Assay [NM_001101] Qiagen, Manchester, UK).

Sanger sequencing

Sanger sequencing in forward and reverse orientations was performed by Source Biosciences (Oxford) using the sequencing primer: 5'-GTT TCC ATT CCA CCA ACA CC-3'.

Statistical analysis

Association data for genotyped and imputed SNPs were obtained on the subset of AS cases of white British ancestry and

white British controls from the recent ImmunoChip GWAS. To evaluate the presence of independent effects on genetic susceptibility at the *RUNX3* locus, we performed conditional analysis on 4230 AS cases and 9700 matched controls, as previously described.¹ Association analysis was performed using the logistic regression function in PLINK (V.1.90),²⁷ accounting for population structure with 10 PCs, and conditioning on the *RUNX3* SNP *rs4648889*.

One-way analysis of variance (ANOVA) and two-tailed Student's t test were used to determine statistical significance using the GraphPad Prism software (V.5.03) package.

RESULTS

Conditional analysis identifies *rs4648889* as a candidate causal variant

The previous AS ImmunoChip study¹ identified *rs6600247* as the lead SNP at the *RUNX3* locus (1.3×10^{-14}), with *rs4648889* as the next most strongly associated SNP ($p = 7.6 \times 10^{-14}$). We performed conditional analysis and found no evidence of independent effects in disease susceptibility between these two SNPs, reflecting the strong LD between them (table 1). After conditioning on SNP *rs4648889*, only two of the other 22 *RUNX3* SNPs previously shown to be strongly associated with AS at $p \leq 10^{-11}$ retained positive ($p < 0.02$) association—*rs4265380* (1.7×10^{-7}) and *rs7529070* ($p = 1.2 \times 10^{-7}$). Conditioning on these two SNPs independently, the strong association with the SNP *rs4648889* was retained ($p \leq 3.0 \times 10^{-6}$ for both SNP), thereby establishing the primacy of this association with AS in this region.

Identification of a regulatory region upstream of *RUNX3* containing *rs4648889*

We first identified a putative regulatory element ~2 kb upstream of the *RUNX3* distal promoter in the region of *rs4648889* (figure 1A). This was based on published DNase I hypersensitivity sites (DHS) in seven cell types, ChIP-seq peaks for TF binding and the presence of both H3K4Me1 and H3K27Ac histone modifications (figure 1A).^{20–28} This regulatory element also contains a DHS site in CD8+ T cells (<http://www.epigenomebrowser.org>) and is predicted to bind several TFs. The region around *rs4648889* is more likely to be functionally relevant than *rs6600247*, the lead SNP in the previous ImmunoChip study, considering the paucity of TF binding near the latter (figure 1B).

We therefore hypothesised that this region is an active enhancer-like element 5' of the *RUNX3* promoter (figure 1).

Differential binding of nuclear extract including IRF4 at *rs4648889*

Analysis of ChIP-seq data from the ENCODE project revealed binding of several TFs to the region surrounding *rs4648889* (figure 1). We investigated the effect of the *rs4648889* dimorphism on TF binding to a 50 bp DNA fragment using EMSA. Addition of nuclear extract from Jurkat cells (leukaemia T-cell line) to this DNA probe created a major protein–DNA complex (i) with a visibly weaker band for the AS-risk allele 'A' (~5.4-fold \pm 1.2 SEM less than 'G') than the AS-protective 'G' allele (figure 2A). Addition of CD8+ T-cell nuclear extract also generated a weaker band for a protein–DNA complex (ii) with the risk 'A' allele (~3.1-fold \pm 1.4 SEM less than 'G') compared with the 'G' allele (figure 2B). In these experiments Jurkat and CD8+ T-cell nuclear extract binding to the 'G' allele was successfully competed by 200-fold and 100-fold excess of unlabelled 'G', but not 'A' probe and vice versa (figure 2A and see online supplementary figure S1A). The strong binding of both Jurkat and CD8+ T-cell nuclear lysates to the AS-protective 'G' allele of *rs4648889* was greatly reduced by adding IRF4 antibody. In contrast, this had little discernible influence on the already very weak binding of either of these nuclear lysates to the AS-risk 'A' allele (figure 2A, B).

This suggests that TFs, including IRF4 in the resulting complex, exhibit allele-specific binding to the region around *rs4648889*.

rs4648889 alters IRF4 binding and H3K4Me1 histone methylation

We used ChIP and allele-specific qPCR to assess DNA binding by IRF4 in *rs4648889* heterozygous CD8+ T cells freshly isolated from three patients with AS. Three independent experiments showed IRF4 was preferentially recruited (threefold increase \pm 1.0 SEM, $p = 0.058$) to the AS-protective 'G' allele compared with the AS-risk 'A' allele (figure 3A).

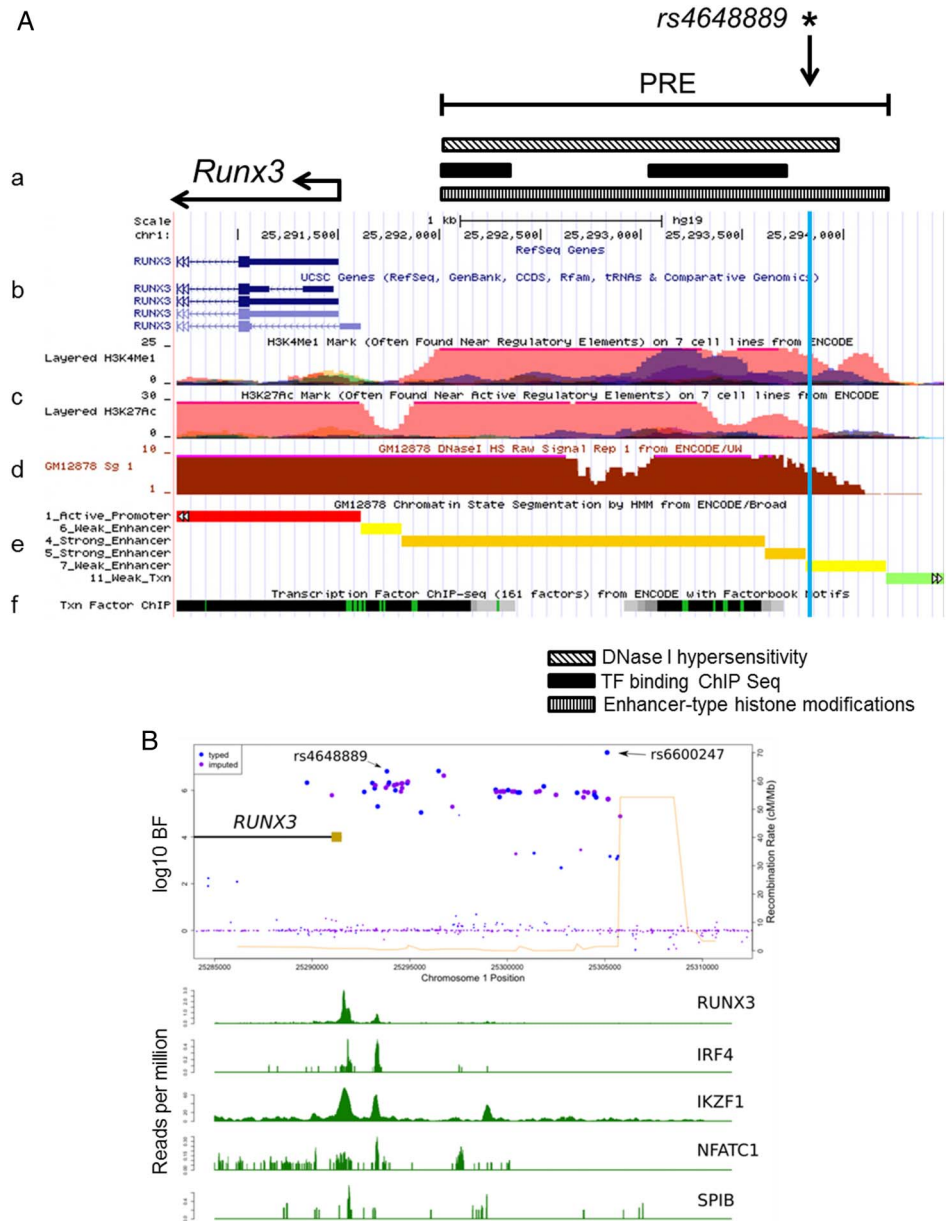
ChIP-seq data from ENCODE identified the 2 kb region upstream of the *RUNX3* promoter as an enhancer region with increased histone H3K4Me1 in seven different cell lines. We therefore conducted ChIP qPCR for H3K4Me1 on CD8+ T

Table 1 Conditional analysis of SNP associations at *RUNX3*

Chr.	SNP	Position*	Risk/non-risk allele	Conditional SNP	p Value	OR	RAF (case–control)	LD (r^2/D') with conditional SNP
1	<i>rs6600247</i>	25177701	C/T	<i>rs4648889</i>	0.9	1.01	0.54/0.51	0.90/0.97
				<i>rs4265380</i>	1.5×10^{-4}	1.64		0.97/1
				<i>rs7529070</i>	4.9×10^{-5}	1.67		0.97/1
1	<i>rs4648889</i>	25166416	A/G	<i>rs6600247</i>	0.2	0.84	0.54/0.50	0.90/0.97
				<i>rs4265380</i>	2.1×10^{-6}	3.96		0.94/1
				<i>rs7529070</i>	3.0×10^{-6}	2.87		0.94/1
1	<i>rs4265380</i>	25165943	T/C	<i>rs6600247</i>	1.0×10^{-6}	0.53	0.55/0.50	0.97/1
				<i>rs4648889</i>	1.7×10^{-7}	0.22		0.94/1
				<i>rs7529070</i>	0.6	1.14		1/1
1	<i>rs7529070</i>	25168167	A/G	<i>rs6600247</i>	2.1×10^{-7}	0.52	0.53/0.50	0.97/1
				<i>rs4648889</i>	1.2×10^{-7}	0.30		0.94/1
				<i>rs4265380</i>	0.3	0.77		1/1

*National Center for Biotechnology Information (NCBI) Build 36 human genome coordinates. Chr., chromosome; LD, linkage disequilibrium; RAF, risk allele frequency; SNP, single nucleotide polymorphism.

Figure 1 Epigenetic and transcriptional landscape of the 2 kb putative regulatory region containing *rs4648889* upstream of the *RUNX3* promoter. (A) Representation of *RUNX3* promoter and putative regulatory element (PRE) location (a). From ENCODE data: *RUNX3* gene location and promoter (b). Histone modification chromatin immunoprecipitation (ChIP)-seq data including H3K4me1 and H3K27Ac (c). DNase I hypersensitivity GM12878 lymphoblastoid cell line (d), predicted chromatin state (e) and condensed transcription factor (TF) ChIP-seq (f) data from various cell lines are shown. (B) *rs4648889* site shows specific TF binding compared with *rs6600247*. ENCODE TF ChIP-seq data from GM12878 lymphoblastoid cell line show differential TF binding between *rs4648889* and *rs6600247* for *RUNX3*, IRF4, IKZF1, NFATC1 and SPIB. Blue and light violet dots represent genotyped and imputed single nucleotide polymorphisms variants and their location; light brown rectangle shows the *RUNX3* promoter.



cells. The AS-protective 'G' allele had >2.5-fold relative enrichment ($p=0.03$) compared with the AS-risk 'A' allele (figure 3B).

Sanger sequencing of one *rs4648889*-heterozygous AS case showed that the 'G' allele was relatively enriched in chromatin fragments immunoprecipitated with antibodies for H3K4Me1 and IRF4 ChIP compared with the reference input (see online supplementary figure S2).

The AS-risk 'A' allele at *rs4648889* shows decreased reporter gene activity

Reporter activity of the region around *rs4648889* was also evaluated in vitro by luciferase reporter assay. The 250 bp region containing *rs4648889* showed increased luciferase activity compared with the minimal promoter (minP=1) but the presence of the AS-risk allele 'A' reduced the enhancer activity from 9.1-fold to 4.3-fold ($p\leq 0.01$) in HEK293T cells (human embryonic kidney cell line) and from 4.0-fold to 1.9-fold ($p\leq 0.01$) in Jurkat cells (figure 4A, B). The same result was observed in Jurkat cells stimulated with phorbol myristate acetate (PMA)/phytohaemagglutinin (PHA) for 24 h (figure 4C). These findings

support the view that the lower enhancer activity at the AS-risk 'A' allele is due to decreased H3K4Me1 occupancy.

The homozygous 'AA' genotype at *rs4648889* is associated with reduced *RUNX3* mRNA levels

Analysis of *RUNX3* expression (figure 5) in CD8+ T cells isolated from patients with AS having different *rs4648889* genotypes (6 GG, 7 AG and 6 AA) showed that *RUNX3* mRNA levels, normalised against β -actin, were significantly lower in subjects with the AA than the GG genotype (1.7 ± 0.9 vs 4.2 ± 2.2 SEM, ANOVA $p\leq 0.05$). No correlation was observed between *RUNX3* expression and disease activity as defined either by BASDAI or CRP.

DISCUSSION

We have shown here that *rs4648889* is probably the primary AS-associated SNP at the *RUNX3* locus and that this association can probably be best explained through its effects on gene expression. The *rs4648889* AS-risk allele 'A' exhibits relatively low luciferase reporter activity compared with the

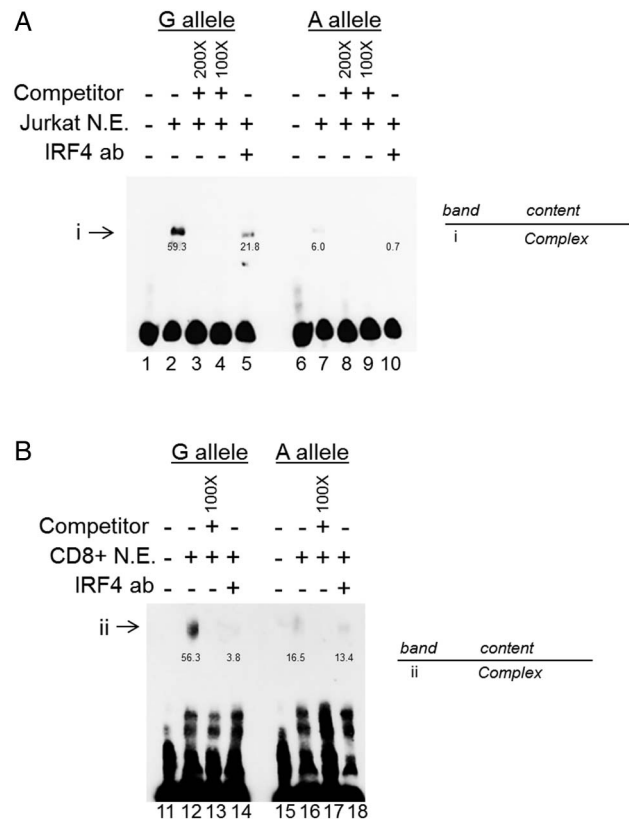


Figure 2 *rs4648889* segment region alters protein–DNA complex formation with evidence of IRF4 involvement. Chemiluminescent electrophoretic mobility gel shift assay (EMSA) (A) showing complex formations (i) after addition of Jurkat nuclear extract (lanes 2 and 7), competition with 200-fold and 100-fold excess of unlabelled probes (lanes 3, 4 and 8, 9) and IRF4 involvement after addition of IRF4 antibody (lanes 5 and 10). IRF4 antibody addition leads to inhibition of the complex (i) (lanes 5 and 10). (B) EMSA showing protein–DNA complex formation (ii) after addition of CD8+ nuclear extract (lanes 12 and 16). IRF4 antibody was used to compete with the labelled oligonucleotides for binding of the nuclear extract (lanes 14–18). Numbers below the bands indicate pixel density. N.E., nuclear extract.

AS-protective ‘G’ allele, less *RUNX3* mRNA levels and less enrichment for H3K4Me1 histone modification of a type associated with active enhancer elements.⁷ The AS-risk allele ‘A’ is also reproducibly associated with reduced formation of protein–DNA complexes that contain IRF4. The TF IRF4 is involved in regulating the number and function of CD8+ T cells,^{29–32} influencing their differentiation, expansion^{30–33} and metabolism.³¹ Our results are consistent with previous reports that selective IRF4 binding to the distal promoter exerts an inhibitory effect on *RUNX3* expression and consequently on CD8+ T-cell development and function.³² Previous studies have indicated that the total number of peripheral blood CD8+ T cells is significantly decreased in AS cases, and that this is strongly correlated with the *RUNX3* genotype.^{1–2} We believe that this may be mediated through differential allelic binding of TF complexes (including IRF4) to this *RUNX3* enhancer. *RUNX3* plays a key role in haematopoiesis and enhances CD8 T-cell development/activation and has an inhibitory effect on CD4+ T cells.^{9–10} *RUNX3* affects NK cell development,¹⁰ mediates transforming growth factor- β responses in the activation of dendritic cells during inflammation³⁴ and, together with T-bet, regulates interferon- γ and interleukin 4 expression in T-helper (Th)1 cells.³⁵

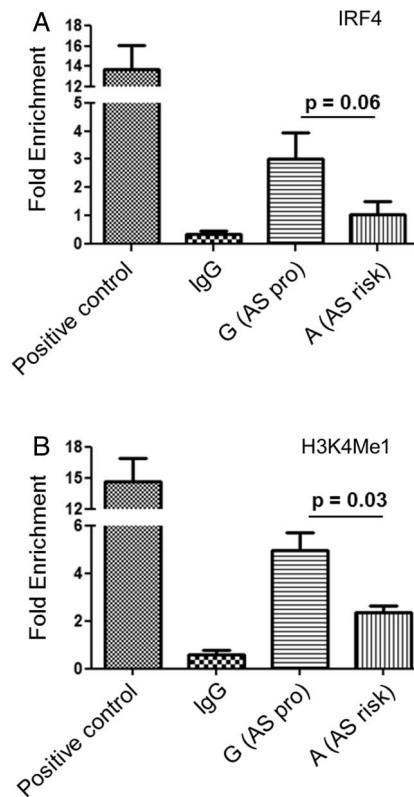


Figure 3 Ex vivo allele-specific binding of IRF4 and H3K4Me1 methylation at the *rs4648889* site. Allele-specific IRF4 (A) and H3K4Me1 (B) chromatin immunoprecipitation (ChIP) quantitative PCR assessed at the *rs4648889* locus in heterozygous CD8+ T cells isolated from three patients with ankylosing spondylitis (AS). The PCR reactions for both the ‘G’ and ‘A’ alleles were done in triplicate in each of the three cases. The relative enrichment is expressed as mean \pm SEM ($p < 0.05$, Student’s t test). Enhancer sequence from *IL10* was used as positive control.

The striking *HLA-B*27* association with AS has long tempted speculation that aberrant immune responses to microbial infection, perhaps mediated through *HLA-B27*-restricted CD8+ cytotoxic T cells, could be involved.^{36–37} Such ideas have been strengthened by the observation that *HLA-B*27*-transgenic rats develop SpA unless reared in germ-free conditions.³⁸ However, *HLA-B*27* transgenic rats still develop SpA in the absence of CD8+ T cells.³⁹ Our results would be consistent with the hypothesis that reduced CD8+ T-cell numbers and/or function play a role in the pathogenesis of AS. More than 40 genetic influences have been identified in AS, several of which (*HLA-B*27*, *RUNX3*, *EOMES*, *TBX21*, *ZMIZ1*, *IL7* and *IL7R*) potentially affect lymphocyte biology.¹ Currently, the full complexity of immune cell involvement in AS is incompletely understood. Here we have demonstrated potential epigenetic regulatory effects at the *RUNX3* locus in CD8+ T cells. We have not yet extended these studies to other cell types, such as Th1, NK, dendritic or other immune cells that could also be involved in AS.⁴⁰ For example, reduced *RUNX3* expression could enhance CD4+ T-cell activity, which would be consistent with models of AS invoking a pathological role for CD4+ T cells.^{41–42} In particular, CD4+ Th17 cells have been implicated in AS and appear to be present in increased numbers in the peripheral blood of patients with pre-radiographical axial SpA⁴³ and reactive arthritis.⁴⁴

It is likely that most genetic associations in AS reflect relatively subtle changes in gene expression. The differences in

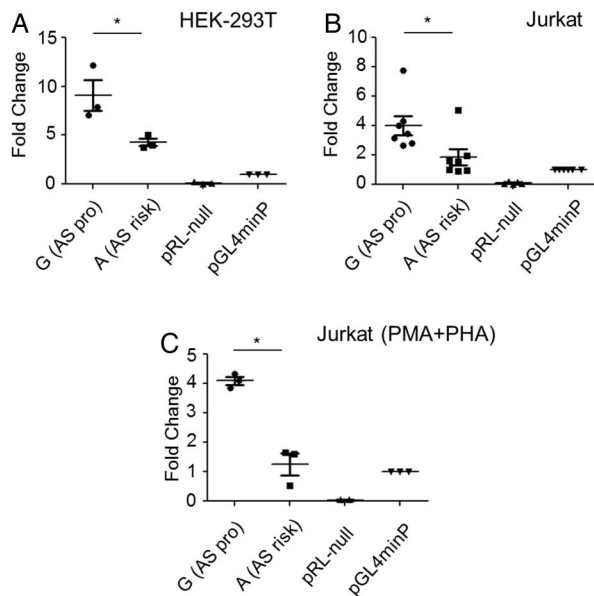


Figure 4 *rs4648889* site shows enhancer activity in vitro. The transcriptional activity of *rs4648889* compared with minimal promoter (minP) was measured by luciferase assays on (A) HEK293T (n=3), (B) Jurkat cells (n=7) and (C) Jurkat cells stimulated with PMA/PHA for 24 h (n=3). The values of relative luciferase activity are expressed as mean±SEM. The relative luciferase activity of the ankylosing spondylitis (AS)-risk 'A' allele was significantly reduced compared with the AS-protective 'G' allele (* $p < 0.01$, Student's t test).

DNA–protein complexes revealed by EMSA experiments between the AS-risk 'A' and AS-protective 'G' allele require further investigation to define the full diversity of TFs involved in these complexes and also the network of genes that might ultimately be regulated by the *rs4648889* polymorphism. It is

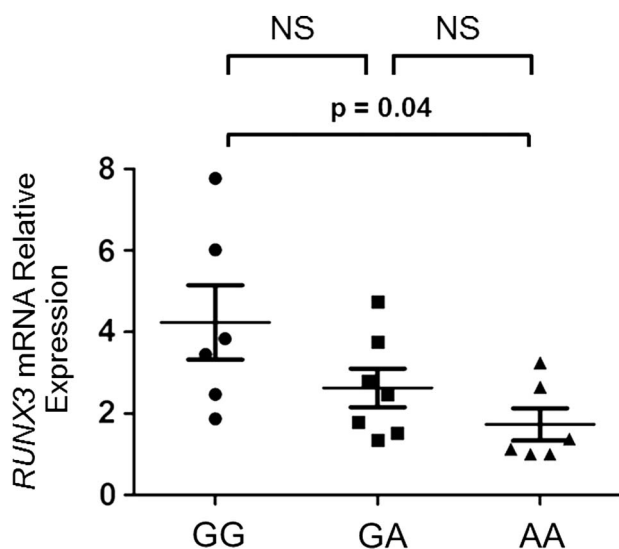


Figure 5 Allele-specific effects of *rs4648889* on RUNX3 expression. Relative amount of *RUNX3* mRNA transcript in primary CD8+ T cells from 19 patients with ankylosing spondylitis having different genotypes was measured by quantitative PCR using the comparative cycle threshold method. The p values were determined using analysis of variance. There was a significant difference ($p = 0.04$) between the GG and the AA homozygotes. The differences between the GA heterozygotes and the GG or AA homozygotes were not significant (NS).

well known that eukaryotic transcription may be controlled by regulatory elements that are distant from their target genes; such control can be exerted (sometimes on multiple genes) through the formation of chromatin loops.^{45 46} We have not formally excluded the possibility that this *RUNX3* regulatory region could influence other more distant genes relevant to AS. Establishing the full extent of the genes (and their regulation) in these pathways and their relationship to the pathogenesis of AS represents a considerable challenge. In future we will investigate TF binding and chromatin accessibility across the whole genome to explore the composition of these AS gene regulatory networks.⁴⁷

This work illustrates the first steps towards a more complete mechanistic understanding of just one of the many genetic associations of AS. These and related techniques have broad applications to the investigation of other similar regulatory polymorphisms that probably account for much of the genetic risk in AS. A deeper knowledge of the factors involved in these processes is likely to lead to the discovery of new therapeutic targets.

Acknowledgements The authors wish to thank all the study participants who generously donated their DNA to this study.

Contributors MV, ARR, CJC, AC, JCK, PB and BPW conceived and designed the experiments. MV, ARR and AC performed the experiments. MV, ARR, CJC, AC, PB and BPW analysed the data. MV, ARR, CJC, AC, PB, JCK and BPW wrote the manuscript.

Funding MV was funded by NIHR Oxford Comprehensive Biomedical Research Centre (immunity and inflammation theme A93081) and ARR by Arthritis Research UK (Grant 20402). Additional funding was provided by Arthritis Research UK (Grants 18797, 19536 and 20796), the NIHR Thames Valley collaborative research network and National Ankylosing Spondylitis Society (UK).

Competing interests None declared.

Patient consent Obtained.

Ethics approval Central Oxford Research Ethics Committee COREC 06/Q1606/139 and OXREC B 07/Q1605/35).

Provenance and peer review Not commissioned; externally peer reviewed.

Open Access This is an Open Access article distributed in accordance with the terms of the Creative Commons Attribution (CC BY 4.0) license, which permits others to distribute, remix, adapt and build upon this work, for commercial use, provided the original work is properly cited. See: <http://creativecommons.org/licenses/by/4.0/>

REFERENCES

- Cortes A, Hadler J, Pointon JP, *et al.*. International Genetics of Ankylosing Spondylitis Consortium (IGAS). Identification of multiple risk variants for ankylosing spondylitis through high-density genotyping of immune-related loci. *Nat Genet* 2013;45:730–8.
- Evans DM, Spencer CC, Pointon JJ, *et al.*. Interaction between ERAP1 and HLA-B27 in ankylosing spondylitis implicates peptide handling in the mechanism for HLA-B27 in disease susceptibility. *Nat Genet* 2011;43:761–7.
- Karaderi T, Harvey D, Farrar C, *et al.*. Association between the interleukin 23 receptor and ankylosing spondylitis is confirmed by a new UK case-control study and meta-analysis of published series. *Rheumatology (Oxford)* 2009;48:386–9.
- Harvey D, Pointon JJ, Evans DM, *et al.*. Investigating the genetic association between ERAP1 and ankylosing spondylitis. *Hum Mol Genet* 2009;18:4204–12.
- Hindorf LA, Sethupathy P, Junkins HA, *et al.*. Potential etiologic and functional implications of genome-wide association loci for human diseases and traits. *Proc Natl Acad Sci USA* 2009;106:9362–7.
- Apel M, Uebe S, Bowes J, *et al.*. Variants in *RUNX3* contribute to susceptibility to psoriatic arthritis, exhibiting further common ground with ankylosing spondylitis. *Arthritis Rheum* 2013;65:1224–31.
- Schaub MA, Boyle AP, Kundaje A, *et al.*. Linking disease associations with regulatory information in the human genome. *Genome Res* 2012;22:1748–59.
- Cohen MM Jr. Perspectives on *RUNX* genes: an update. *Am J Med Genet* 2009; 149:2629–46.
- Lotem J, Levanon D, Negrœanu V, *et al.*. Runx3 at the interface of immunity, inflammation and cancer. *Biochim Biophys Acta* 2015;1855:131–43.
- Levanon D, Negrœanu V, Lotem J, *et al.*. Transcription factor Runx3 regulates interleukin-15-dependent natural killer cell activation. *Mol Cell Biol* 2014;34:1158–69.

- 11 Sugai M, Aoki K, Osato M, *et al.* Runx3 is required for full activation of regulatory T cells to prevent colitis-associated tumor formation. *J Immunol* 2011;186: 6515–20.
- 12 Taniuchi I, Osato M, Egawa T, *et al.* Differential requirements for Runx proteins in CD4 repression and epigenetic silencing during T lymphocyte development. *Cell* 2002;111:621–33.
- 13 Cruz-Guilloty F, Pipkin ME, Djuretic IM, *et al.* Runx3 and T-box proteins cooperate to establish the transcriptional program of effector CTLs. *J Exp Med* 2009;206:51–9.
- 14 Rini D, Calabi F. Identification and comparative analysis of a second RUNX3 promoter. *Gene* 2001;273:13–22.
- 15 Bangsow C, Rubins N, Glusman G, *et al.* The RUNX3 gene sequence, structure and regulated expression. *Gene* 2001;279:221–32.
- 16 Han H, Cortez CC, Yang X, *et al.* DNA methylation directly silences genes with non-CpG island promoters and establishes a nucleosome occupied promoter. *Hum Mol Genet* 2011;20:4299–310.
- 17 Paluszczak J, Sarbak J, Kostrzewska-Poczekaj M, *et al.* The negative regulators of Wnt pathway-DACH1, DKK1, and WIF1 are methylated in oral and oropharyngeal cancer and WIF1 methylation predicts shorter survival. *Tumour Biol* 2015;36:2855–61.
- 18 Estécio MR, Maddipoti S, Bueso-Ramos C, *et al.* RUNX3 promoter hypermethylation is frequent in leukaemia cell lines and associated with acute myeloid leukaemia inv (16) subtype. *Br J Haematol* 2015;169:344–51.
- 19 Guo C, Ren F, Wang D, *et al.* RUNX3 is inactivated by promoter hypermethylation in malignant transformation of ovarian endometriosis. *Oncol Rep* 2014;32:2580–8.
- 20 ENCODE Project Consortium. A user's guide to the encyclopedia of DNA elements (ENCODE). *PLoS Biol* 2011;9:e1001046.
- 21 Delaneau O, Zagury JF, Marchini J. Improved whole chromosome phasing for disease and population genetic studies. *Nat Methods* 2013;10:5–6.
- 22 Abecasis GR, Auton A, Brooks LD, *et al.*, 1000 Genomes Project Consortium. An integrated map of genetic variation from 1,092 human genomes. *Nature* 2012;491:56–65.
- 23 Howie B, Fuchsberger C, Stephens M, *et al.* Fast and accurate genotype imputation in genome-wide association studies through pre-phasing. *Nat Genet* 2012;44:955–9.
- 24 Howie BN, Donnelly P, Marchini J. A flexible and accurate genotype imputation method for the next generation of genome-wide association studies. *PLoS Genet* 2009;5:e1000529.
- 25 Van der Linden S, Valkenburg HA, Cats A. Evaluation of diagnostic criteria for ankylosing spondylitis. A proposal for modification of the New York criteria. *Arthritis Rheum* 1984;27:361–8.
- 26 Garrett S, Jenkinson T, Kennedy LG, *et al.* A new approach to defining disease status in ankylosing spondylitis: the Bath Ankylosing Spondylitis Disease Activity Index. *J Rheumatol* 1994;21:2286–91.
- 27 Purcell S, Neale B, Todd-Brown K, *et al.* PLINK: a tool set for whole-genome association and population-based linkage analyses. *Am J Hum Genet* 2007;81:559–75.
- 28 ENCODE Project Consortium. An integrated encyclopedia of DNA elements in the human genome. *Nature* 2012;489:57–74.
- 29 Lotem J, Levanon D, Negraru V, *et al.* Runx3-mediated transcriptional program in cytotoxic lymphocytes. *PLoS ONE* 2013;8:e80467.
- 30 Yao S, Buzo BF, Pham D, *et al.* Interferon regulatory factor 4 sustains CD8(+) T cell expansion and effector differentiation. *Immunity* 2013;39:833–45.
- 31 Man K, Miasari M, Shi W, *et al.* The transcription factor IRF4 is essential for TCR affinity-mediated metabolic programming and clonal expansion of T cells. *Nat Immunol* 2013;14:1155–65.
- 32 Cao Y, Li H, Sun Y, *et al.* Interferon regulatory factor 4 regulates thymocyte differentiation by repressing Runx3 expression. *Eur J Immunol* 2010;40:3198–209.
- 33 Nayar R, Schutten E, Bautista B, *et al.* Graded levels of IRF4 regulate CD8+T cell differentiation and expansion, but not attrition, in response to acute virus infection. *J Immunol* 2014;192:5881–93.
- 34 Fainaru O, Woolf E, Lotem J, *et al.* Runx3 regulates mouse TGF-beta-mediated dendritic cell function and its absence results in airway inflammation. *EMBO J* 2004;23:969–79.
- 35 Collins PL, Chang S, Henderson M, *et al.* Distal regions of the human IFNG locus direct cell type-specific expression. *J Immunol* 2010;185:1492–501.
- 36 Fiorillo MT, Maragno M, Butler R, *et al.* CD8(+) T-cell autoreactivity to an HLA-B27-restricted self-epitope correlates with ankylosing spondylitis. *J Clin Invest* 2000;106:47–53.
- 37 Schirmer M, Goldberger C, Würzner R, *et al.* Circulating cytotoxic CD8(+) CD28(–) T cells in ankylosing spondylitis. *Arthritis Res* 2002;4:71–6.
- 38 Taurag JD, Richardson JA, Croft JT, *et al.* The germfree state prevents development of gut and joint inflammatory disease in HLA-B27 transgenic rats. *J Exp Med* 1994;180:2359–64.
- 39 Taurag JD, Dorris ML, Satumtira N, *et al.* Spondylarthritis in HLA-B27/human beta2-microglobulin-transgenic rats is not prevented by lack of CD8. *Arthritis Rheum* 2009;60:1977–84.
- 40 Chan AT, Kollnberger SD, Wedderburn LR, *et al.* Expansion and enhanced survival of natural killer cells expressing the killer immunoglobulin-like receptor KIR3DL2 in spondylarthritis. *Arthritis Rheum* 2005;52:3586–95.
- 41 Overgaard NH, Jung J, Steptoe RJ, *et al.* CD4+/CD8+ double-positive T cells: more than just a developmental stage? *J Leukoc Biol* 2015;97:31–8.
- 42 Boyle LH, Goodall JC, Gaston JS. The recognition of abnormal forms of HLA-B27 by CD4+ T cells. *Curr Mol Med* 2004;4:51–8.
- 43 Jansen DT, Hameetman M, van Bergen J, *et al.* IL-17-producing CD4+ T cells are increased in early, active axial spondyloarthritis including patients without imaging abnormalities. *Rheumatology (Oxford)* 2015;54:728–35.
- 44 Shen H, Goodall JC, Gaston JS. Frequency and phenotype of T helper 17 cells in peripheral blood and synovial fluid of patients with reactive arthritis. *J Rheumatol* 2010;37:2096–9.
- 45 Ghousaini M, Edwards SL, Michailidou K, *et al.* Evidence that breast cancer risk at the 2q35 locus is mediated through IGFBP5 regulation. *Nat Commun* 2014;4:4999.
- 46 Huang Q, Whittington T, Gao P, *et al.* A prostate cancer susceptibility allele at 6q22 increases RFX6 expression by modulating HOXB13 chromatin binding. *Nat Genet* 2014;46:126–35.
- 47 Ciofani M, Madar A, Galan C, *et al.* A validated regulatory network for Th17 cell specification. *Cell* 2012;151:289–303.

Supplementary Methods

The genetic association of *RUNX3* with ankylosing spondylitis can be explained by allele-specific effects on IRF4 recruitment that alter levels of gene expression

Matteo Vecellio^{1,2,3}, Amity R Roberts^{1,2,3}, Carla J Cohen^{1,2,3}, Adrian Cortes^{4,5}, Julian C Knight⁵, Paul Bowness^{1,2,3} and B Paul Wordsworth^{1,2,3}

Author affiliations

¹Nuffield Department of Orthopaedics, Rheumatology and Musculoskeletal Sciences, University of Oxford, Oxford, UK

² National Institute for Health Research Oxford Musculoskeletal Biomedical Research Unit, Oxford, UK

³ National Institute for Health Research Oxford Comprehensive Biomedical Research Centre, Botnar Research Centre, Nuffield Orthopaedic Centre, Oxford, UK

⁴Nuffield Department of Clinical Neurosciences, Division of Clinical Neurology, John Radcliffe Hospital, University of Oxford, Oxford, UK

⁵Wellcome Trust Centre for Human Genetics, Roosevelt Drive, University of Oxford, Oxford, UK

Address for correspondence:

Prof BP Wordsworth

NIHR Oxford Musculoskeletal Biomedical Research Unit,

Botnar Research Centre,

Nuffield Orthopaedic Centre

Windmill Road,

Headington,

Oxford

OX3 7LD

Email: paul.wordsworth@ndorms.ox.ac.uk

Telephone: 44 (0)1865741155

Luciferase Reporter Assay

In details, HEK293T and Jurkat cells were cultured in DMEM and RPMI, respectively, supplemented with 10% fetal bovine serum (FBS), 100 units/ml penicillin/ streptomycin and 2 mM L-glutamine. 200,000 HEK293T or Jurkat cells/well in 96/24-well plates, were co-transfected with 100/500 ng of pGL4 construct and 2/10 ng of pRL-null (Promega, Madison, USA) using GeneJuice (Novagen, Darmstadt, Germany) and GeneIN™ (GlobalStem, Gaithersburg, USA) respectively. After 24 hours transfection, Jurkat cells were stimulated with PMA/PHA (1 µg/ml PHA + 50 ng/ml PMA, Sigma Aldrich, Gillingham, UK) for 16 hours. After 48 hours in total, luciferase activity was measured using the Dual-Luciferase assay reporter system (Promega, Madison, USA). Firefly luciferase activity was normalized relative to Renilla luciferase activity for each transfection and calculated as fold increase over pGL4.23[luc2/minP].

Student *t*-test and one-way ANOVA were used to determine significant differences between the two allelic constructs.

Electrophoretic Mobility Gel Shift Assay (EMSA)

Briefly, EMSA were performed as follows: incubations were done at room temperature for 40 minutes in total. IRF4 Antibody (Santa Cruz Biotechnology, Dallas, USA sc-377383, 5 µg) was added to the nuclear extract (Jurkat or CD8+ T-cells) for 20 minutes, followed by DNA for additional 20 min. Reactions were run chilled on pre-cast non-denaturing 6% DNA retardation gels (Invitrogen, Paisley, UK) with 0.5-fold TBE running buffer (45 mM Tris, 45 mM boric acid, 1 mM EDTA, pH 8.0).

DNA was then transferred at 380 mA from the gel to a pre-activated nitrocellulose membrane for 30 to 60 minutes on ice and cross-linked by UV. All blocking and detection incubations were performed according to manufacturer's instructions (Thermo Scientific, Waltham, USA) and the membrane was exposed to X-ray film.

The sequence of the DNA probes are:

rs4648889 Forward, A allele: 5'-CCT GAG GGG CTT CCC CCT CCC TGG A*AA CCT GAG TCC AGG CCC AGG AAG G-3',

rs4648889 Reverse, A allele: 5'-CCT TCC TGG GGC CTG GAC TCA GGT TT*C CAG GGA GGG GGA ACC CCT CAG G-3';

rs4648889 Forward, G allele: 5'- CCT GAG GGG CTT CCC CCT CCC TGG G*AA CCT GAG TCC AGG CCC AGG AAG G-3',

rs4648889 Reverse, G allele: 5'- CCT TCC TGG GGC CTG GAC TCA GGT TC*C CAG GGA GGG GGA ACC CCT CAG G -3'.

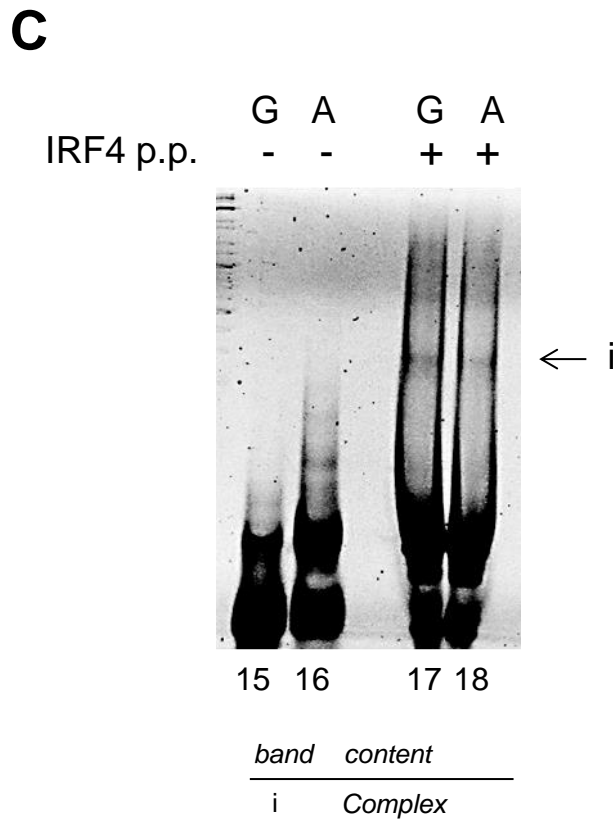
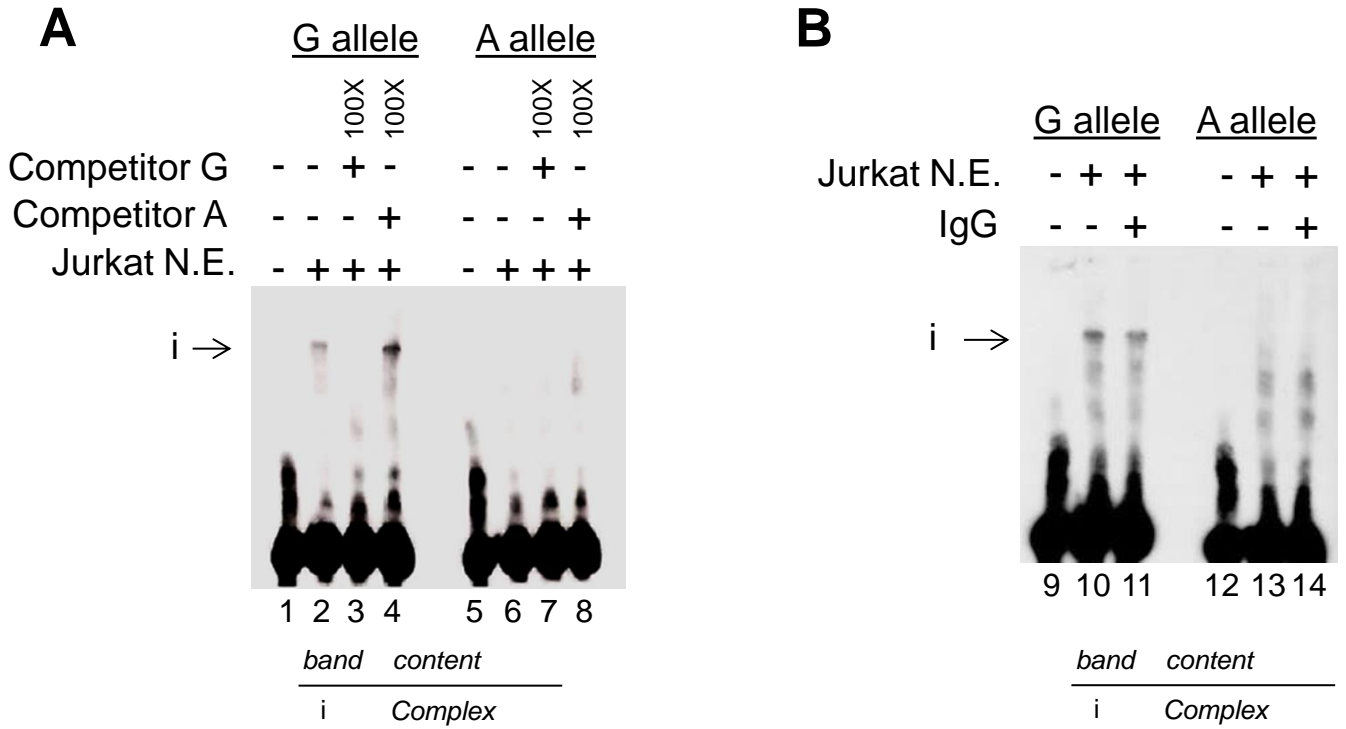
The stars highlight the *rs4648889* position.

Suppl. figure 1: *rs4648889* segment region alters protein/DNA complex formation confirming IRF4 involvement and specificity. (A) Representative chemiluminescent EMSA showing competition experiments with 100 fold excess of unlabelled competitor for both alleles (lanes 3, 4, 7 and 8). (B) Effect of nonspecific IgG antibody addition (lanes 11 and 14). (C) Representative EMSA showing binding for IRF4 purified protein, with preference for the AS-protective allele “G” (lanes 17 and 18).

Suppl. figure 2: Sanger sequencing after ChIP-qPCR of H3K4Me1 and IRF4. ChIP followed by sequencing for the *rs4648889*-containing region in heterozygous CD8+ T-cells from AS patients. Chromatograms represent one ChIP experiment generated and sequenced. Levels of H3K4Me1 and IRF4 are relatively higher for the protective “G” allele, compared to the risk “A” allele, after normalization on input.

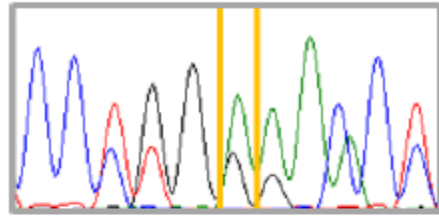
Suppl. figure 3: IRF4 protein expression in cell lines used in reporter assay and EMSA. (A) Western blot analysis showing IRF4 protein expression: 51 kDa band was detected in HEK 293T, Jurkat and Raji cell lines. Band density is reported in the associated bar graph (n= 3 for each group). (B) Real-Time PCR showing IRF4 mRNA expression in HEK 293T, Jurkat and Raji cell lines (n=2, in triplicate).

Supplementary Figure 1



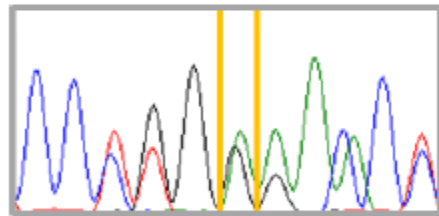
Supplementary Figure 2

Exp 1



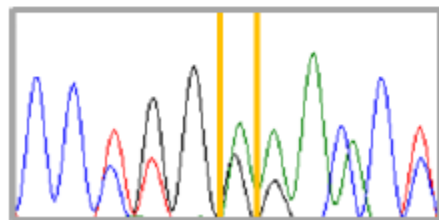
Input

G/A



H3K4Me1

G/A

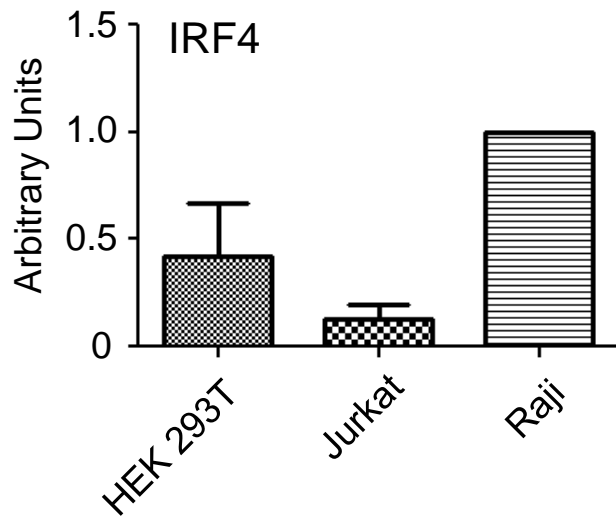
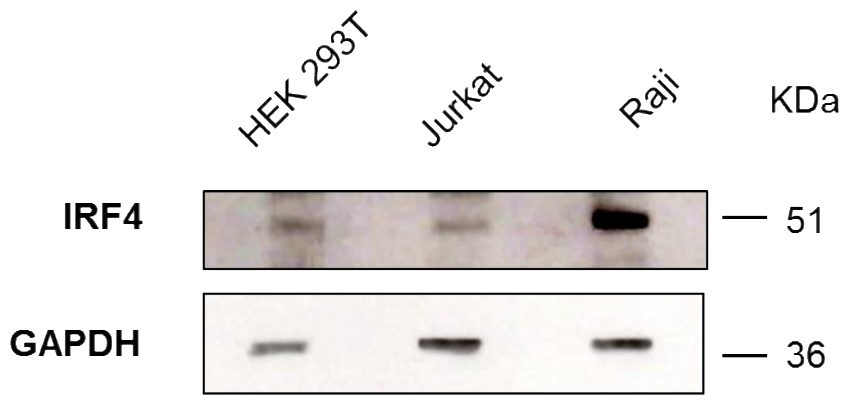


IRF4

G/A

Supplementary Figure 3

A



B

